Nuclear Engineering and Technology 49 (2017) 141–147

Available online at ScienceDirect

Nuclear Engineering and Technology

journal homepage: www.elsevier.com/locate/net

Original Article

Research on Mechanical Shim Application with Compensated Prompt γ Current of Vanadium Detectors

Zhi Xu

Suzhou Nuclear Power Research Institute, Xihuan Road 1788, Suzhou, Jiangsu 215004, PR China

ARTICLE INFO

Article history:
Received 30 March 2016
Received in revised form
19 August 2016
Accepted 22 August 2016
Available online 13 October 2016

Keywords:
Lead Lag
Mechanical Shim
Prompt γ Current
Response Time
Robust
Sensitivity
Vanadium Detectors

ABSTRACT

Mechanical shim is an advanced technology for reactor power and axial offset control with control rod assemblies. To address the adverse accuracy impact on the ex-core power range neutron flux measurements-based axial offset control resulting from the variable positions of control rod assemblies, the lead-lag-compensated in-core self-powered vanadium detector signals are utilized. The prompt γ current of self-powered detector is ignored normally due to its weakness compared with the delayed β current, although it promptly reflects the flux change of the core. Based on the features of the prompt γ current, a method for configuration of the lead-lag dynamic compensator is proposed. The simulations indicate that the method can improve dynamic response significantly with negligible adverse effects on the steady response. The robustness of the design implies that the method is of great value for engineering applications.

1. Introduction

Westinghouse (Westinghouse Electric Company LLC, 1000 Westinghouse Drive Suite 572A Cranberry Township, PA 16066) has developed an advanced technology, called "mechanical shim" (MSHIM), to control the reactor power and axial power offset with control rod assemblies alone. This technology satisfies the utility requirements document's need of load-following operation without adjusting the boron concentration. It has been (will be) applied to System 80+ (Palo Verde Nuclear Generating Station, Tonopah, Arizona, in western Arizona, USA), the third-generation passive safety reactor (AP1000), and small module reactor (IRIS) [1–3]. Without the need for adjusting boron concentration for both load-following and load-regulation operations, MSHIM controls the movement of rod assemblies instead, resulting in significant reduction of radioactive liquid waste release. However, the operational mode with the frequent movement of control rods significantly impacts the traditional core power protection and axial power offset control method that is based on the calibrated ex-core power measurements [4,5]. Normally, vanadium detectors are used to provide very precise in-core nuclear power distribution. However, response of the vanadium detector with a delay of more than 10 minutes [6] prevents its application for axial offset control directly. The lead-lag algorithm can be used for the delayed time response

E-mail address: xuzhi@cgnpc.com.cn.
http://dx.doi.org/10.1016/j.net.2016.08.015

compensation, hereby the compensated signal can be applied to tune the prompt, ex-core power-based axial offset control [7]. In fact, in-core vanadium detectors produce both β current and prompt γ current. Because of vanadium detectors' weak prompt γ current flow compared with β current flow, it is usually ignored. A dedicated design of the lead-lag unit to compensate the delayed β signal current and utilize prompt γ current to obtain fast response with negligible steady-state errors is presented in this paper. In addition, MATLAB/Simulink numerical simulations are carried out to verify the performance of the design.

2. Axial offset control of MSHIM and its compensation

Constant axial offset control requires the in-core nuclear power constant ratio of the sum of the top half and bottom half to the deviation between them, so the change of power will inevitably lead to the axial offset change. Usually, the top and bottom power measurements are obtained using the ex-core power range top and bottom detectors [1–3,8]. For most operations in the traditional second-generation pressurized water reactors, the control rods are almost withdrawn out of the active core area (all rods out), and move very infrequently, leading to a uniform core power distribution. However, frequent movement of control rod assemblies in the MSHIM strategy breaks the consistency between the ex-core and in-core axial offset. The withdrawal of rod assemblies results in the upward tilt of axial offset, whereas the insertion of rod assemblies leads to the downward tilt of axial offset. Moreover, the ex-core detectors are sensitive to the fuel assembles in the face peripheral area, intensifying the possible deviations between ex-core-measured axial offset and the actual in-core axial offset. Fig. 1 [5] presents the correlations of the ex-core measurement-based axial offset (AO_{ex}) versus the peripheral fuel assembly-based axial offset (AO_{wp}) and core axial offset (AO_{in}). Because of the significant deviation between the core axial offset and the ex-core-measured axial offset, the protection system uses the calibrated axial offset based on ex-core-weighted peripheral fuel assemblies [4,5]. The protection system transmits the calibrated signal to the control system for the axial offset control, which might limit reactor power or operational capability.

Benefits offered by vanadium self-powered neutron detectors (SPNDs), such as a better life span, simple response characteristics, and easiness in handling the replaced SPNDs, make them desirable candidates for in-core flux distribution mapping applications. For instance, there are evenly configured 42 self-powered vanadium detector assemblies, with each composed of seven purified ^{51}V, in the core. The longest detector is the length of the core active area, the rest of the six detectors reduce the length by one-seventh from the longest one [1–3]. The position of vanadium detectors in an assembly is shown in Fig. 2 [7].

Based on the good consistency of the in-core vanadium detectors' current flow with the nuclear power, in addition to the specified layout in the core, the ΔØ of in-core power deviation of top and bottom half by detectors located in j area is expressed as follows:

$$\Delta\varnothing = \left(P_j^T - P_j^B\right) = K_j^c\left(I_{4j} + I_{5j} - I_{1j}\right) \tag{1}$$

where K_j^c represents the factor for the c^{th} detector located in the j area, and I_{cj} is the current flow output from the c^{th} detector located in the j area.

To correlate with the four power deviation signals from the four divisions of the protection system, the 42 detector assemblies are grouped into four quadrants. The IAP_i represents power deviation for the i^{th} quadrant.

$$IAP_i = m_{ai}\left(\frac{1}{N_i}\sum_{j=1}^{N_i} I_{4j} + \frac{1}{M_i}\sum_{j=1}^{M_i} I_{5j} - \frac{1}{P_i}\sum_{j=1}^{P_i} I_{1j}\right) + b_{ai} \tag{2}$$

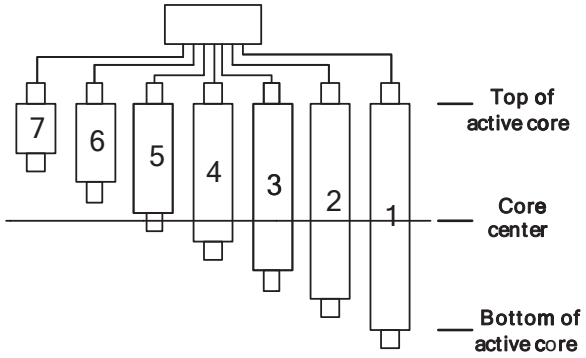

Fig. 2 – Configuration of vanadium detectors in an assembly.

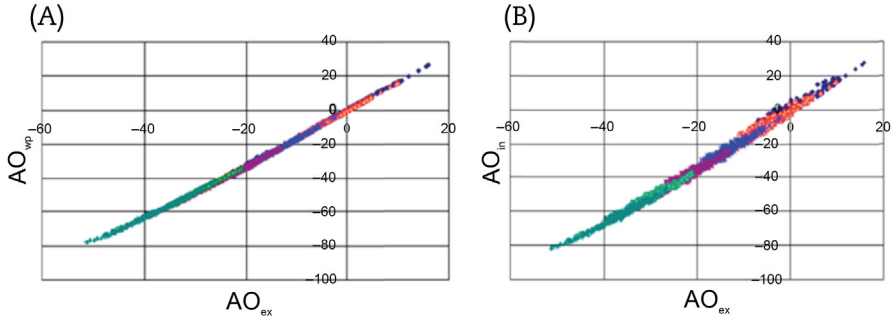

Fig. 1 – (A) Peripheral fuel assembly-based axial offset (AO_{wp}) and (B) core axial offset (AO_{in}) versus ex-core measurement-based axial offset (AO_{ex}).

where N_i, M_i, and P_i represent the available detector numbers of 4th, 5th, and 1st in quadrant i respectively. m_{ai}, b_{ai} is the linear fitting factor for the steady power deviation based on other systems, that is, online power distribution monitoring system.

As shown in Fig. 1, the MSHIM operating mode results in a significant inconsistency between the calibrated measurements (AFD_i^{WP}) based on peripheral fuel assembly and the core axial offset; meanwhile, the axial offset control system receives these AFD_i^{WP} for axial offset control. Xu [7] has presented a method for tuning AFD_i^{WP} with time delay-compensated IAP_i accompanied by amplitude limiters.

$$\Delta a_i(t) = \frac{1}{N+1}\sum_{j=0}^{N}\left[IAP_i(t-j) - AFD_i^{WP}(t-j-\tau)\right] \quad (3)$$

$$AFD_i(t) = \begin{cases} AFD_i^{WP}(t) + \Delta a_i(t), |\Delta a_i(t)| - |\delta_{ai}(t)| < 0 \\ AFD_i^{WP}(t) + \delta_{ai}(t), |\Delta a_i(t)| - |\delta_{ai}(t)| \geq 0 \end{cases} \quad (4)$$

where N is the counting numbers falling in the average window for stability improvement, τ is the time difference between compensated signals and the corresponding signals from ex-core, and $\delta_{ai}(t)$ is the predefined limiter. The simulations indicate the method is of good efficiency, however, the performance of method depends on the features of the time-delay compensation and the proper selection of τ.

3. Time delay compensation for vanadium detectors

3.1. Current flow generated by vanadium detectors

The vanadium (^{51}V) detector has the features of simple structure, small size, exempt of high-voltage offset, low burnup, and typical 1/V neutron response, and is deployed in nuclear power plants widely. The current flow generated by vanadium detectors is the composition of three effects. A neutron is captured in the emitter of vanadium via the formation of a capture product isotope, which decays by β emission—99.2% of this emission has endpoint energy of 2.5404 MeV [9]. Normally, 42% of the β emission is energetic enough to escape from the vanadium and the insulator, producing a current flow that is proportional to the neutron flux [10]. Neutron capture in the aforementioned vanadium method is always accompanied by the emission of prompt capture γ rays. Whole or parts of the γ-rays' energy are absorbed by the vanadium through interactions, by releasing electrons via Compton, photo-electric process, and pair production. Some electrons are energetic enough to escape from the vanadium and the insulator, and thus produce a current flow. In the early 1980s, many studies [11–13] on using γ signals from SPNDs were carried out. Because of gamma background from fission products and the poor conversion efficiency, the current flow for this part is ignored normally [14]. The incident γ ray from a reactor to detector itself generates Compton, pair production, and photo-electrons, with some being energetic enough to produce a current flow. Although this incident γ-induced current flow is prompt, because approximately 50% of this γ flow is delayed in a power reactor, it cannot follow flux changes simultaneously. Consequently [10,15], regard these γ-induced current flow as interference. Fig. 3 shows the three primary mechanisms by which incident radiation, including neutron and γ are converted to energetic electrons.

Normally, only the current generated by β interactions is considered, therefore

$$I(t) = K\sigma_a eN\left(1 - e^{-\frac{0.693t}{T_{1/2}}}\right)\varnothing \quad (5)$$

where K, σ_a, e, N, and $\varnothing$ represent the material factor, thermal activation cross section, electronic factor, atomicity of vanadium, thermal neutron flux; $T_{1/2}$ represents the half-life of vanadium.

As shown in Eq. 5, the generated current flow by a detector is proportional to the neutron flux when t approaches infinity (∞). Although ^{52}V has a half-life of 225 s, due to the fact that the material of detectors is not made of 100% pure vanadium, the vanadium detectors' response time constant for neutron flux rate upon step inputs is 326 s [16]. In other words, the detector output current flow reaches 63% of the final value in 326 s. The features of detectors can be expressed by

$$W_1(s) = \frac{1}{326s+1} \quad (6)$$

where s is the variable of Laplace transform. Fig. 4 shows the time response upon the step flux change.

3.2. Brief review of current compensation methods

As shown in Fig. 4, the time required to achieve steady (93% of the final value) output of vanadium detectors is about 15 minutes, which restricts their application in nuclear power plants. Normally, the vanadium detectors are used for in-core flux distribution calculations. To facilitate the advantages of the detectors, many compensation algorithms are developed. Typical compensation algorithms are inverse function [6], Kalman filtering [17], H_∞ filtering [18], software with computer sampling [19], and latest filtering [20,21]. A lead-lag compensator is normally used in a control system that improves an undesirable frequency response in a feedback and control system. The properly configured lead-lag unit can improve the dynamic response and noise immunity so well that it is deployed for control systems in a nuclear power plant. In considering the rather simple neutron response feature of vanadium detectors, the cost of those algorithms, and the dynamic response characteristics of lead-lag unit [22], the lead-lag-based compensation unit following the detectors

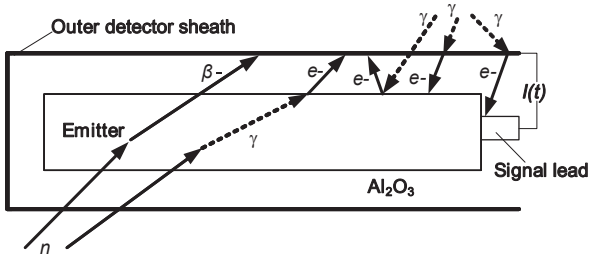

Fig. 3 – Neutron and γ interactions within a vanadium detector.

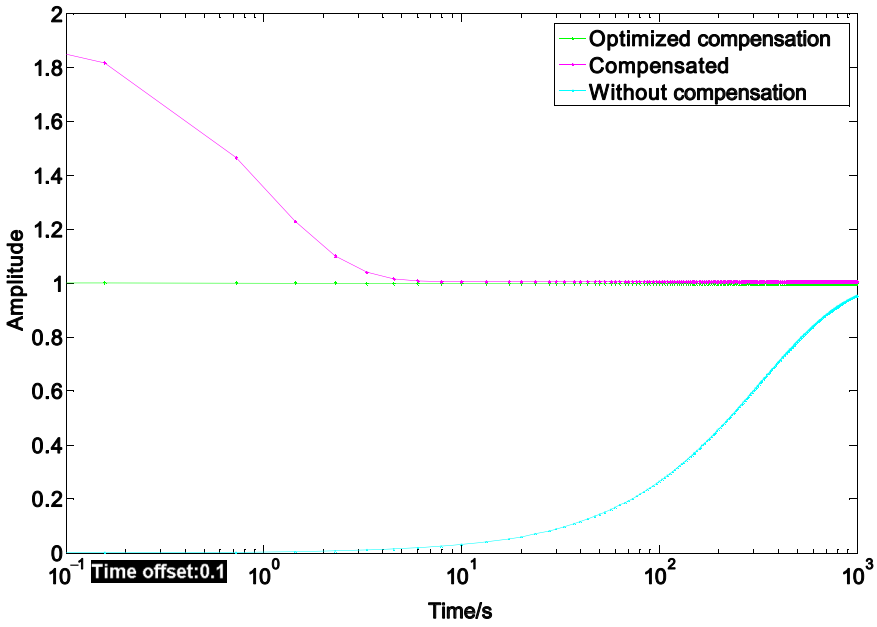

Fig. 4 – Response to neutron flux step stimulation.

immediately is deployed to get faster overall response time. Xu [7] designed the lead-lag unit as follows:

$$W_2(s) = \frac{326s + 1}{s + 1} \tag{7}$$

Fig. 4 shows the outputs of vanadium detectors following lead-lag compensation upon the unit step flux changes. Although the inputs to the lead-lag compensation are digitalized, for simplicity, the continuous model is used in the simulations with the conservative input variances, which are unlikely conditions in operations.

3.3. *Optimized compensation*

As Li [15] points out, although the γ-induced current of detectors is small, it should be removed by the thermal neutron sensitivity calibration in specific conditions and the method for the γ- and β-induced current flow sensitivity identification should be given. Product specifications from Sweden KWD nuclear instruments indicate the thermal neutron β current flow is 0.51 μA, whereas the γ-induced current flow is 0.007 μA, under the condition of 10^{14} n/cm^2/s thermal neutron flux rate. Therefore, theγ-induced current flow is 1.4% of the total current flow. William [23] also points out the γ-induced current occupies about 1% of the overall current flow generated. Normally, it is regarded that about 50% of the γ-induced energy is generated by prompt γ [8]; in addition to the poor conversion efficiency, the effect of (*n*, γ, *e*) for the detector itself can be ignored. Thus, it is regarded, that approximately 50% of γ-induced current is generated via (γ, *e*) incident prompt γ, which reflects the neutron flux change simultaneously. The following lead-lag compensation algorithm is designed to utilize these valuable dynamic current signals.

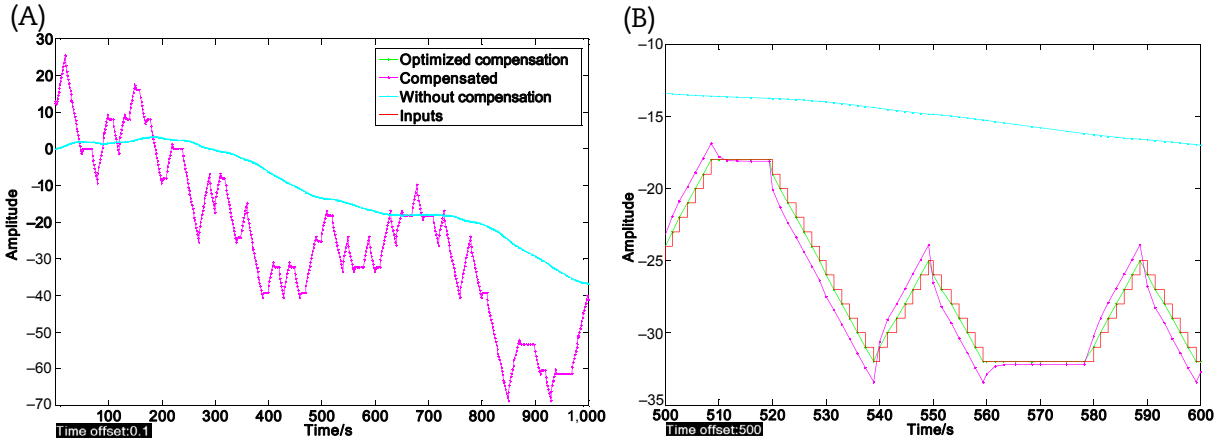

Fig. 5 – Random inputs stimulations. (A) Response to random inputs stimulations. (B) Magnified view of response to random inputs stimulation.

Taking the prompt γ current that occupies K% of the total current flow into consideration, the current feature for detectors can be expressed as $W_{1o}(s) = \frac{1}{326\ s+1} + K/100$. To get the expected performance, set the lead-lag unit W_o (s) as

$$W_o(s) = \frac{(326s+1)(100-K)}{3.26K(100-K)s+100} \tag{8}$$

The system's overall transfer function Y(s) is thus

$$Y(s) = \left(K/100 + \frac{1}{326s\ +\ 1}\right) \frac{(326s\ +1)(100-K)}{3.26K(100-K)s\ +100} \tag{9}$$

When there is unit step flux change in-core as input, there is $Y(\infty) = 1$. Based on mirror features of the time and frequency domains, the output in time domain is

$$y(0) = 1 \tag{10}$$

Likewise, $Y(0) = 1 - K^2/10,000$, which means the output in time domain is

$$y(\infty) = 1 - K^2/10,000 \tag{11}$$

Normally, the K is very small, then $y(\infty) \approx 1$.

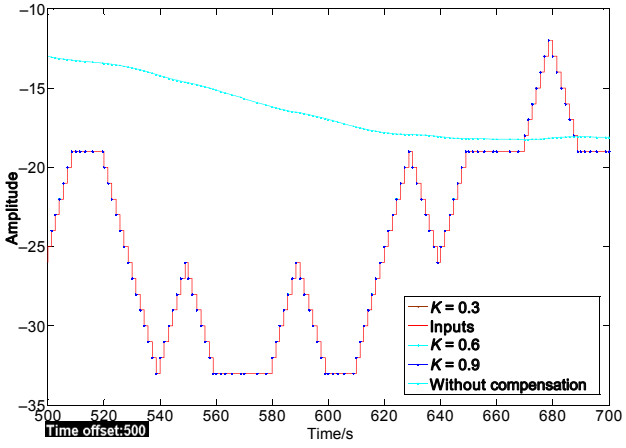

Fig. 6 – Response of detectors with different Ks upon random inputs stimulations

4. Simulations and analysis

All the following examples are calculated using MATLAB/Simulink to verify the performance of the proposed method.

The output in respective situation without compensation, compensated with $W_2(s) = \frac{326s+1}{s+1}$, and with the aforementioned optimized method using $W_o(s) = \frac{(326s+1)(100-K)}{3.26K(100-K)s+100}$, where $K = 0.6$, upon the unit step stimulus, is shown in Fig. 4.

The simulation indicates that the optimized compensation utilizing the prompt γ-current flow signals has tremendous advantages beyond the former compensation in terms of dynamic response.

Assuming the inputs are of random characteristics, that is, the probability of unit step change, negative unit step change, and without change are the same, the overall output without compensation, with compensation, and the optimized compensation are shown in Fig. 5A. The magnified details for part of the simulation are shown in Fig. 5B.

Fig. 5 shows that the virgin system without any compensation has a strong low-pass filter characteristic and does not follow the inputs well; consequently, the loss of high-frequency signals is too much to be accepted. The compensated method, however, has a much better response, although there are some overshoots. The system response with optimized compensation follows the inputs quite well and has significant advantages over the others in terms of both dynamic and steady features.

Fig. 6 shows the minor differences among different Ks, that is, 0.3, 0.6, and 0.9 respectively, which indicate that the method can be deployed widely.

As shown in Fig. 7, the response of using incorrect parameters in two limiting situations for compensation does not degrade the performance to an unacceptable level, which indicates that the optimized compensation method is of parameter (K) robustness.

Fig. 8A shows the situation when the input is contaminated by noise at the front end, that is, in-core. Fig. 8B shows the situation when the electrical noise is induced in the late section, that is, in the cables carrying the current flow to the signal processing equipment. Because of the feature of large

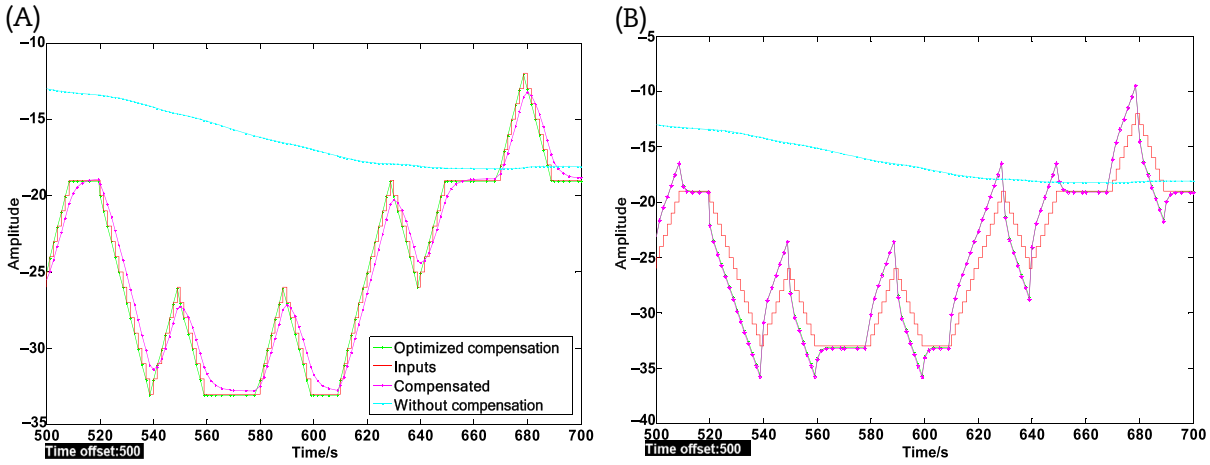

Fig. 7 – (A) Response of a detector of $K = 0.3$ upon random inputs calculated with $K = 0.9$. (B) Response of a detector of $K = 0.9$ upon random inputs calculated with $K = 0.3$.

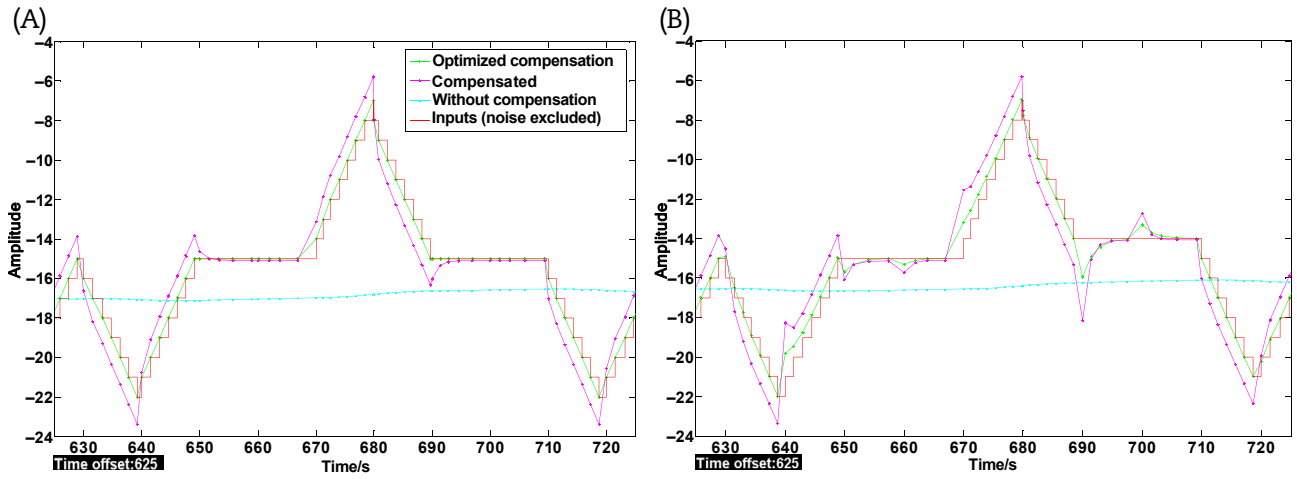

Fig. 8. – (A) Response to inputs with noise injected at the front end. (B) Response to inputs with noise injected at the late end.

time constant low-pass filters for the detectors, the front end-induced noise has little effects on the output. Fig. 8B indicates that the late end-induced noise degrades the performance significantly for both the referenced and optimized compensation. In either case, the latter has preferred performance over the formal method for it follows the input closer. For AP1000, the signal processing equipment connected with detectors immediately is installed inside the containment and very close to the reactor vessel, which contains all the detectors. The dedicated cables from detectors to the equipment further minimize the potential signal contamination [1–3].

It should be noted that Eq. (5) is of approximate accuracy. The temperature-related isolation resistance impacts the actual current from detectors. Studies by Yu [14], Yang et al [16], and Moreira and Lescano [24] have demonstrated that the temperature affects the measured current flow from vanadium detectors. Rao and Misra [25] indicated that neutron sensitivity of vanadium detectors should take into account additional factors, namely, flux depression caused by detectors and the interaction of gamma rays, which result in the correction factors that have been evaluated to be 0.957 and 1.03, respectively, for the specific detectors. In fact, normally, the temperature for detectors in the core and the temperature measurement vary slowly. From an engineering viewpoint, the calibration of detectors in time, can take into account all the aforementioned facts, leading to an expected precision. Meanwhile, the time constant of detectors might vary a little for specific manufacturers. It can be justified and replaced instead of using the time constant of 326 s utilized in this paper if required.

5. Conclusion

With the combination of characteristics of the lead-lag dynamic compensation and normally neglected prompt γ current flow of vanadium detectors, a method for the lead-lag compensator configuration based on the real prompt γ detector current occupancy is proposed. Numerical simulations show that the method can significantly improve the detectors' dynamic response, upon step and random stimulus inputs. Because of much faster time response for this optimized compensation, in combination with the method [7] for adjusting axial offset control in the MSHIM mode, a much better overall system performance can be expected, with the direct configuration of τ as zero in Eq. (3). This method also provides the possibility of using the optimized compensated vanadium current signals only for the axial offset control. The occupancy robustness for detectors' prompt γ current flow implies that the method is of significant engineering advantages. How to get the occupancy proportion of the individual detector's prompt γ current flow conveniently for best performance is the key focus for upcoming studies.

Conflicts of interest

The author has no conflicts of interest to declare.

Acknowledgments

The author greatly appreciates the financial support of National Science and Technology Major Project grant funded by the Chinese government (Grant No. 2014ZX06907-002).

REFERENCES

[1] C.G. Lin, Z.S. Yu, Passive Safety Advanced Pressurized Water Reactor Technology, Atomic Energy Press, Beijing, 2008.
[2] H.H. Sun, P.D. Cheng, H.X. Miu, W.Z. Zhang, X.G. Zhu, M.H. Weng, Third Generation Nuclear Power Technology AP1000, China Electric Power Press, Beijing, 2010.
[3] L.L.C. Westinghouse, Westinghouse AP1000 Design Control Document, Westinghouse Electric Company LLC, Pittsburgh (PA), 2012.
[4] C. Xing, Y. Zhang, Z. Zheng, Control and monitoring of AP1000 constant axial offset, East China Electr. Power 2 (2013) 0420–0423.
[5] R. Wang, Y. Zhou, Correction of ex-core nuclear instrumentation measurement in mechanical shim mode, Electr. Instrum. Customers 5 (2013) 93–95.

[6] Z.Y. Xiao, Z.S. Yang, Inverse function amplifier for self-powered detectors, Nucl. Power Eng. 5 (1982) 30–35.
[7] Z. Xu, Design of axial offset control with compensated vanadium detectors, At. Energy Sci. Technol. 50 (2016) 524–530.
[8] J.L. Pu, Guangdong Daya Bay Nuclear Power Plant Running Tutorial, Atomic Energy Press, Beijing, 1999.
[9] National Nuclear Data Center [Internet]. Information extracted from the NuDat 2 database. Available from: http://www.nndc.bnl.gov/nudat2/. (Accessed 15 August).
[10] W.Z. Liu, S.C. Li, Z.X. Hu, Z.M. Tang, Q. Yang, The introduction of self-powered detector and study for its escape probability calculation algorithm for β particle, Nucl. Electron. Detect. Technol. 1 (2015) 5–7.
[11] H. Weiss, Experimental Comparison between In-core Gamma Radiation and Neutron Flux Density Distribution in a Pressurized Water Reactor, Westinghouse Electric Corporation, Pittsburgh (PA), 1970.
[12] J.J. Loving, Neutron, temperature, and gamma sensors for pressurized water reactors, IEEE Trans. Ind. Electron. Control Instrum IECI-17 (1970) 120–129.
[13] O. Strindehag, Self-powered Neutron and Gamma Detectors for In-core Measurements, Ab. Atomenergi, [Rapp.] AE AE-440, 1971, pp. 1–18.
[14] Y.M. Yu, Properties of long vanadium self-powered detector, Nucl. Tech. 1 (1980) 15–19, 27.
[15] K.M. Li, The application of self-powered detectors in intensive γ core, Nucl. Sci. Eng. 3 (1983) 359–365.
[16] Y.N. Yang, W.Z. Wang, J.H. Sun, D.J. Zhou, Flexible vanadium self-powered detectors, Nucl. Electron. Detect. Technol. 2 (1983) 21–28.
[17] M.L. Kantrowitz, An improved dynamic compensation algorithm for rhodium self-powered neutron detectors, IEEE Trans. Nucl. Sci. 34 (1987) 562–566.
[18] M.G. Park, Y.H. Kim, K.H. Cha, M.K. Kim, H_∞ filtering for dynamic compensation of self-powered neutron detectors—a linear matrix inequality based method, Ann. Nucl. Energy 26 (1999) 1669–1682.
[19] S.C. Li, L.T. Xiao, Research of delayed response elimination algorithm for rhodium self-powered detectors, Nucl. Electron. Detect. Technol. 29 (2009) 1516–1519.
[20] X.J. Peng, Q. Li, W.B. Zhao, H.L. Gong, K. Wang, Robust filtering for dynamic compensation of self-powered neutron detectors, Nucl. Eng. Des. 280 (2014) 122–129.
[21] X.J. Peng, Q. Li, K. Wang, Dynamic compensation of vanadium self-powered neutron detectors based on Luenberger form filter, Prog. Nucl. Energy 78 (2015) 190–195.
[22] Z. Xu, Q. Bao, Analysis on the response time testing of OTΔT/OPΔT protection for PWR, Nucl. Tech. 38 (2015) 040606-1–040606–7.
[23] H.T. William, Characteristics of self-powered neutron detectors used in power reactors, Proceedings of a Specialists' Meeting, Mito-shi, Japan, 14–17 October,1996. Session 4: Instrumentation. pp. 1–10. https://www.oecd-nea.org/science/rsd/ic96/4-2.pdf.
[24] O. Moreira, H. Lescano, Analysis of vanadium self-powered neutron detector's signal, Ann. Nucl. Energy 58 (2013) 90–94.
[25] P.S. Rao, S.C. Misra, Neutron sensitivity of vanadium self-powered neutron detectors, Nucl. Instr. Meth. Phys. Res. A 253 (1986) 57–60.